

© 2023 IEEE. Personal use of this material is permitted. Permission from IEEE must be obtained for all other uses, in any current or future media, including reprinting/republishing this material for advertising or promotional purposes, creating new collective works, for resale or redistribution to servers or lists, or reuse of any copyrighted component of this work in other works.

# Reconfigurable Intelligent Surface Assisted NOMA Collaborative Localization

D. Zhang<sup>1</sup>, Y. Zhu<sup>1</sup>, G. Cao<sup>1</sup>, M. Li<sup>1\*</sup>, Z. Lu<sup>2</sup> and H. Yuan<sup>3</sup>

<sup>1</sup> School of Electronics Information Engineering, Taiyuan University of Science and Technology, China.  
Email:{S202115110178, s202215110490, S202115110191}@stu.tyust.edu.cn and meilingli@tyust.edu.cn\*

<sup>2</sup> School of Information and Comms. Engineering, Beijing University of Posts and Telecommunications, China.  
Email:lzy0372@bupt.edu.cn

<sup>3</sup> School of Computer Science and Mathematics, Kingston University, KT1 2EE, UK.  
Email:h.yuan@kingston.ac.uk

**Abstract**—This paper proposed a novel integrated localization and communication framework, where reconfigurable intelligent surface-assisted non-orthogonal multiple access simultaneously transmits the communication and localisation signals via line-of-sight links. The bit error rate (BER) performance for communication users and the localization performance for localization users in terms of code phase estimation error (CPEE) and tracking error of the delay locked loop (DLL) are analyzed. The approximate closed forms for BER, CPEE and tracking error of the DLL are derived under Rayleigh fading channels. Finally, the Monte-Carlo simulations are used to validate the analysis. The results show that RIS-NOMA can enhance communication and localization performance compared to NOMA-only. Significantly, the corresponding performance values, i.e. BER, CPEE and tracking error of the DLL, decrease with the number of reflecting elements.

**Index Terms**—integrated localization and communication, RIS, NOMA, BER, code phase estimation error, DLL tracking error

## I. INTRODUCTION

One of the aims of the sixth generation (6G) mobile communication networks toward 2030 is to provide ubiquitous wireless intelligence with high operational flexibility and autonomy and intelligent context-aware services for users [1]. To this end, the 6G wireless system will provide accurate and reliable localization service and enhanced ubiquitous communications simultaneously [2]. Especially in recent years, integrated localization and communication (ILAC) using non-orthogonal multiple access (NOMA) and reconfigurable intelligent surface (RIS) technologies have been extensively investigated to improve wireless localization performance.

The authors in [3], [4] designed a multiscale multiple-input multiple-output non-orthogonal multiple access (MIMO-NOMA) systems to achieve a continuous positioning reference signal (PRS). The authors in [5] further proposed a novel mmWave MIMO-NOMA-based localization system, which shows that the proposed model can reduce position error bound.

The authors in [6] recently demonstrated that the non-line-of-sight (NLoS) transmission might impact the localization performance. RIS has been envisioned that it can be used to drastically enhance the link quality [7]–[12]. The authors in

[7] introduced RIS into the wireless localization system to make the positioning more accurate and energy efficient. The authors in [8]–[10] investigated the RIS-aided ILAC systems for mm-Wave MISO/MIMO, where the beam-forming and localization are analyzed. The authors in [11] analyzed the Fisher information matrix and Cramer–Rao lower bound for the RIS-aided ILAC system. The authors in [13] provided the theoretical framework for comparing the RIS and relay systems, where the outage probability is analyzed. Further, the authors in [14] investigated the integration of RIS and NOMA under imperfect channel state information, where the spectrum efficiency is evaluated. The authors in [15] also studied the outage performance for the RIS-NOMA-aided ILAC system.

Motivated by the above discussion, the communications and localization performance still need further investigation. Differ from [14] and [15], we consider a RIS-assisted NOMA collaborative localization scheme, where the interference between localization signal and communication signal in RIS-NOMA assisted localization system is analyzed. Not only the approximate closed-form expressions of the bit error rate (BER) for communication users are derived, but also the code phase estimation error (CPEE) and the tracking error of delay locked loop (DLL) for locating users under Rayleigh fading channels are analyzed. The Monte-Carlo simulation is used to validate the analysis. The results show that the proposed RIS-NOMA-aided localization scheme can reduce the BER for communication users, the CPEE and the DLL tracking error. Significantly, the communication and localization performance can be simultaneously improved by increasing the number of reflecting elements of the RIS.

## II. SYSTEM MODEL

This paper considers a typically integrated localization and communication framework, which can be used when a communication user cannot receive line-of-sight (LoS) signals due to building obstruction. The downlink transmission system consists of a base station (BS) and a RIS with  $N$  reflecting elements. We assume that the communication user and locating user are in the NLoS area of BS. The BS transmits the superimposed signal  $z = \sqrt{a_c P_s} x_c + \sqrt{a_p P_s} x_p$  to commu-

nication users  $u_c$  and locating users  $u_p$ , where  $u_c$  and  $u_p$  share the communication spectrum using a power domain NOMA transmission scheme to achieve superposition of the localization and communication signal. Let  $P_s$  denote the transmit power,  $a_c$  and  $a_p$  denote the corresponding power allocation coefficient,  $a_c + a_p = 1$ . To ensure the quality of communication services and reduce the interference of the localization signal to the communication signal, the localization signal is allocated in lower power, i.e.  $a_c > a_p$ . When the BS sends a downlink NOMA signal, the communication user and the locating user will receive a superimposed signal which consists of both  $x_c$  and  $x_p$  signals. Therefore, the user  $u$ ,  $u \in (u_c, u_p)$  receives the reflected signal from the RIS can be expressed as

$$y_n = \mathbf{g}_{in}^T \mathbf{\Phi} \mathbf{h}_{bi} z + n_s, \quad (1)$$

where  $n_s \sim CN(0, N_0)$  is the additive white Gaussian noise (AWGN),  $\mathbf{\Phi} = \text{diag}(e^{j\phi_1}, e^{j\phi_2}, \dots, e^{j\phi_N})$ ,  $j = \sqrt{-1}$  is the RIS's diagonal phase shift matrix,  $\beta_n \in [0, 1]$  and  $\phi_n, n = 1, 2, \dots, N$  be the  $n$ -th amplitude reflection coefficient and phase shift, respectively. Let  $\mathbf{h}_{bi} = [h_1, h_2, \dots, h_N]^T$  and  $\mathbf{g}_{in} = [g_1, g_2, \dots, g_N]^T$  be the channel coefficients of the communication links during BS to RIS and RIS to the user, respectively.

### III. PERFORMANCE ANALYSIS

In the considered RIS-NOMA localization system, the pseudo-random code signal is modulated on the localization subcarrier to realise extended gain and distance measurement. The communication signal will be interfered with by the localization signal due to the spectrum leakage caused by the phase discontinuous of the periodic sampling localization signal at the transmitting and receiving nodes, which comes from the non-synchronize between sampling frequency and localization signal frequency. Therefore, the communication performance will be affected by the localization signal. In what follows, the BER is used to measure the communication reliability performance of the user. On the other hand, considering the continuity of the localization signal, we use the CPEE to measure the interference of the communication signal to the localization signal and the tracking error of DLL to evaluate the tracking performance. Thusly, the location performance of the locating user can be obtained.

#### A. BER performance of the communication user

Let  $I_p$  denote the interference intensity to the communication signal due to the leakage of the localization signal spectrum. When the localization signal power is far lower than the noise, the interference to the communication signal by the localization signal can be ignored. Otherwise, it cannot be ignored. We define  $\Delta f_p$  and  $\Delta f_c$  as the carrier spacing of the localization and communication signals, respectively. It is noted that the bandwidth of the localization signal should be wider than the communication one to satisfy the localization and ranging accuracy. Therefore, we consider that  $\Delta f_p = G\Delta f_c$ ,  $G \in N^+$  denotes the multiple of the locating

user subcarrier interval to the communication user subcarrier interval. For an individual location user. According to [8], the  $I_p$  can be expressed as

$$I_p = a_p P_s T_p \sin^2 c^2 \left(1 - \frac{1}{G}\right), \quad (2)$$

where  $T_p$  denotes the symbol period of the localization signal,  $\text{sinc}(x)$  is the strong user. According to the decoding principle of NOMA, communication user  $u_c$  as a strong user uses the successive interference cancellation (SIC) to decode the signal of weak user  $u_p$ , then removes the signal  $x_p$  to decode its signal further. According to (1) and (2), the achievable SNR for communication user  $u_c$  decoding its signal  $x_c$  can be given by

$$\gamma_c = \frac{\beta^2 A^2 a_c P_s}{\beta^2 A^2 a_p P_s + N_0 + I_p}, \quad (3)$$

we assume that the BPSK modulation is utilized. Then, the BER for the communication user can be expressed as

$$BER = \frac{1}{2} \text{erfc} \sqrt{\gamma_c}. \quad (4)$$

From (3), we can see that  $\gamma_c$  varies with the wireless channel fading coefficients. As RIS is used, the LoS link can be realized. Then, we consider all the channels between two nodes following the Rayleigh fading, i.e.  $h_i$  and  $g_i$  are Rayleigh fading channels. According to [15], the channel coefficients can be maximised when the RIS uses the optimal continuous phase shift. Let  $A = |\mathbf{g}_{in}^T \mathbf{\Phi} \mathbf{h}_{bi}| = \left| \sum_{i=1}^N g_i h_i e^{j\phi_i} \right|$  in (2), when RIS using the optimal continuous phase shift, we have  $A = |\mathbf{g}_{in}^T \mathbf{\Phi} \mathbf{h}_{bi}| = \sum_{i=1}^N |g_i| |h_i|$ . Then, (3) can be simplified as

According to [19], the probability density function (PDF) of  $A^2$  can be expressed as

$$f_{A^2}(x) = \frac{1}{2b^{a+1}\Gamma(a+1)} x^{\frac{a-1}{2}} \exp\left(-\frac{\sqrt{x}}{b}\right), \quad (5)$$

where  $a = \frac{k_1^2}{k_2} - 1$ ,  $b = \frac{k_2}{k_1}$ ,  $k_1 = \frac{\pi}{2}\sigma^2 N$ ,  $k_2 = 4N\sigma^4 \left(1 - \frac{\pi^2}{16}\right)$ ,  $\sigma$  is the average Rayleigh fading coefficient. Substituting (5) into (4), we can obtain the statistical average BER for communication users as

$$\begin{aligned} \overline{BER} &= E \left[ \frac{1}{2} \text{erfc} \sqrt{\gamma_c} \right] \\ &= \frac{1}{2} \int_0^\infty \text{erfc} \sqrt{\frac{\beta^2 x a_c P_s}{\beta^2 x a_p P_s + N_0 + I_p}} \times f_{A^2}(x) dx, \end{aligned} \quad (6)$$

Using  $\text{erfc} \approx \frac{1}{\sqrt{\pi}} e^{-\beta^2}$ , (6) can be reviewed as

$$\begin{aligned} \overline{BER} &\approx \frac{1}{2} \int_0^\infty \frac{1}{\sqrt{\pi}} \exp\left(-\frac{\beta^2 x a_c P_s}{\beta^2 x a_p P_s + N_0 + I_p}\right) \\ &\quad \times \frac{1}{2b^{a+1}\Gamma(a+1)} x^{\frac{a-1}{2}} \exp\left(-\frac{\sqrt{x}}{b}\right) dx, \end{aligned} \quad (7)$$

Then, (7) can be further simplified as

$$\overline{BER} \approx \frac{1}{2\sqrt{\pi}b^{a+1}\Gamma(a+1)} \times \int_0^\infty x^a \exp\left[-\left(\frac{\beta^2 x a_c P_s}{\beta^2 x a_p P_s + N_0 + I_p} + \frac{x}{b}\right)\right] dx, \quad (8)$$

It is not easy to get the exact closed forms of the formula (8). We use the Gauss-Laguerre quadrature to get the approximate results of (8). Using  $\int_0^\infty f(x) e^{-x} dx \approx \sum_{i=1}^m \omega_i f(x_i)$  into (8), then we can get

$$\overline{BER} \approx \frac{1}{2\sqrt{\pi}b^{a+1}\Gamma(a+1)} \times \sum_{i=1}^m \eta_i y_i^a \exp\left(y_i - \frac{\beta^2 y_i^2 a_c P_s}{\beta^2 y_i^2 a_p P_s + N_0 + I_p} - \frac{y_i}{b}\right). \quad (9)$$

where, the weight of  $\eta_i$  and points of  $y_i$  can be obtained from [16].

### B. Localization performance of localization user

According to [3], since communication signals and localization signals are transmitted in superposition, communication user signals can interfere with the ranging performance of localization user signals. In NOMA, user  $u_p$  directly decodes its signal by treating the signal of user  $u_c$  as interference. The Signal-to-noise ratio (SNR) of user  $u_p$  can be expressed as

$$\gamma_p = \frac{\beta^2 A^2 a_p P_s}{\beta^2 A^2 a_c P_s + N_0}. \quad (10)$$

The following subsections will analyse the localization performance for localization users regarding CPEE and DLL tracking errors.

1) *CPEE*: We also assume BRSK modulation is used for the localization signal, and then the lower bound of the CPEE in the AWGN channel can be expressed by

$$\sigma_{LB}^2 = 0.25a_1 T_p^2 \frac{r_{cp}}{\gamma_p} \left(B_{fe} - \frac{\gamma_p}{\gamma_p + 1} B\right)^{-1}, \quad (11)$$

where  $a_1$  is determined by the loop parameters,  $B$  is the band width.  $r_{cp} = k \frac{a_c}{a_p}$  is defined as the communication-to-localization ratio, where  $k = 2G - 1 \approx 2G$  represents the number of communication users over one localization user's bandwidth.  $B_{fe}$  is the radio frequency front-end bandwidth.

From (11), we can see that  $\gamma_p$  varies randomly with the channel. Based on Section A, combining (5) and (11), we can obtain a lower bound for the statistical average CPEE of the localized user as

$$\begin{aligned} \overline{\sigma_{LB}^2} &= E[\sigma_{LB}^2] \\ &= \int_0^\infty 0.25a_1 T_p^2 \frac{r_{cp}}{\beta^2 x a_c P_s} (\beta^2 x a_p P_s + N_0) \\ &\quad \times \left(B_{fe} - \frac{\beta^2 x a_c P_s}{\beta^2 x P_s + N_0} B\right)^{-1} f_{A^2}(x) dx, \end{aligned} \quad (12)$$

substituting (5), (6) and (11) into (12), we have

$$\begin{aligned} \overline{\sigma_{LB}^2} &= \frac{0.5a_1 T_p^2 b^{a-1}}{2b^{a+1}\Gamma(a+1)} \\ &\quad \times \int_0^\infty \frac{(\beta^2 b^2 x^2 a_p P_s + N_0) (x^{a-2} \exp(-x))}{\beta^2 a_c P_s} \\ &\quad \times \left(B_{fe} - \frac{\beta^2 x a_c P_s B}{\beta^2 x P_s + N_0}\right)^{-1} dx, \end{aligned} \quad (13)$$

same with (8), we use the Gauss-Laguerre orthogonal method to approximate the integral, and then we can get the approximate expression of the lower bound of the CPEE as

$$\begin{aligned} \overline{\sigma_{LB}^2} &= \frac{0.5a_1 T_p^2 b^{a-1} r_{cp}}{2b^{a+1}\Gamma(a+1)} \sum_{i=1}^m \omega_i x_i^{a-2} \frac{\beta^2 b^2 x_i^2 a_p P_s + N_0}{\beta^2 a_c P_s} \\ &\quad \times \left(B_{fe} - \frac{\beta^2 x_i a_c P_s B}{\beta^2 x_i P_s + N_0}\right)^{-1}. \end{aligned} \quad (14)$$

2) *Tracking error of DLL*: On the other side, DLL tracking error can be used to evaluate the signal tracking performance in multipath fading scenarios [3]. The performance expression can be given as

$$\sigma_t^2 = 0.25a_1 T_p^2 \left[ \frac{2}{B_{fe} T_p \hat{\gamma}_p} + \frac{B}{B_{fe}^2} r_{cp} (\beta_1 + \overline{P_c}) \right], \quad (15)$$

where  $\hat{\gamma}_p = \frac{\beta^2 A^2 a_p P_s}{N_0}$  denotes as the carrier-to-noise ratio of the localization signal,  $\overline{P_c}$  is the normalized power of the communication signal at the receiver. Particularly if there are no multi-path signals, i.e.,  $\beta_1 = 1$ ,  $\overline{P_c} = 0$  [3].

We can see that  $\hat{\gamma}_p$  varies randomly with the channel in (15). Based on Section A, combining (5) and (15), we can obtain the DLL tracking error in the AWGN channel is

$$\begin{aligned} \overline{\sigma_t^2} &= E[\sigma_t^2] = \int_0^\infty 0.25a_1 T_p^2 \\ &\quad \times \left[ \frac{2}{B_{fe} T_p \frac{\beta^2 x a_p P_s}{N_0}} + \frac{B}{B_{fe}^2} r_{cp} (\beta_1 + \overline{P_c}) \right] f_{A^2}(x) dx, \end{aligned} \quad (16)$$

Substituting (5), (6) and (15) into (16), we have

$$\begin{aligned} \overline{\sigma_t^2} &= \frac{1}{2b^{a+1}\Gamma(a+1)} \left[ \frac{a_1 T_p^2 N_0 b^{a+1}}{B_{fe} T_p \beta^2 a_p P_s} \right. \\ &\quad \times \int_0^\infty x^{a-2} \exp(-x) dx + \frac{2B(\beta_1 + \overline{P_c}) r_{cp} b^{a+1}}{B_{fe}^2} \\ &\quad \left. \times \int_0^\infty x^a \exp(-x) dx, \right] \end{aligned} \quad (17)$$

Let  $I_1 = \int_0^\infty x^{a-2} e^{-x} dx$ ,  $I_2 = \int_0^\infty x^a e^{-x} dx$  and using  $\Gamma(s) = \int_0^\infty e^{-x} x^{s-1} dx$ , then  $I_1 = \Gamma(a-1)$ ,  $I_2 = \Gamma(a+1)$ . Substituting  $I_1$ , and  $I_2$  into (17), we have

$$\begin{aligned} \overline{\sigma_t^2} &= \frac{1}{2b^{a+1}\Gamma(a+1)} \left[ \frac{a_1 T_p^2 N_0}{B_{fe} T_p \beta^2 a_p P_s} b^{a-1} \Gamma(a-1) \right. \\ &\quad \left. + \frac{B}{B_{fe}^2} r_{cp} (\beta_1 + \overline{P_c}) 2b^{a+1} \Gamma(a+1) \right]. \end{aligned} \quad (18)$$

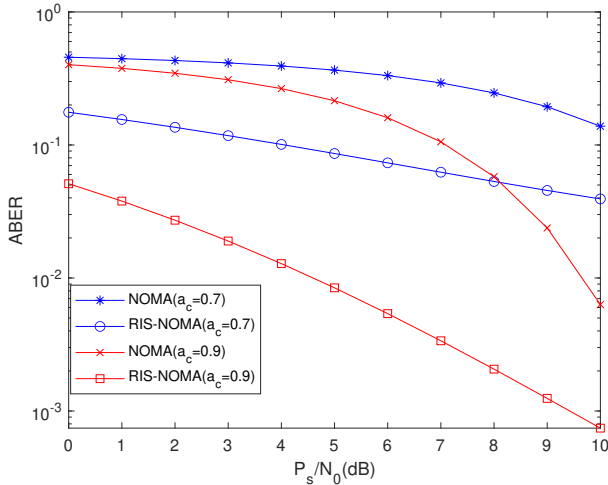


Fig. 1. Average BER vs SNR under the two schemes: RIS-NOMA and NOMA-only.

#### IV. SIMULATION RESULTS

In this section, we evaluate the proposed RIS-NOMA signal's performances from the BER and range measurement accuracy, respectively. We compare the RIS-NOMA localization system with the NOMA-only localization system. We assume that both communications and localization users use BPSK modulation. We also assume that the communication signal is 50 times faster than the localization signal, i.e.  $G = 50$ . Unless otherwise cited, we let  $\sigma = 0.6$ ,  $N = 8$  and  $T_p = \frac{1}{1500}$ ,  $B_{fe} = 2B$  and  $B = 30MHz$  in this paper.

In Fig. 1, the average BER performance vs transmit SNR for communication users are illustrated under RIS-NOMA and NOMA-only schemes. We can see that the BER performance gradually decreases with the increase of SNR. This is because the more significant SNR, the better the quality of the communication signal and the lower the BER. Meanwhile, we found that the BER under the RIS-NOMA scheme decreases faster with the increase of SNR than that of the NOMA-only scheme. We can also see that When  $a_c = 0.7$ ,  $a_p = 0.3$ ,  $r_{cp} = 24dB$ , and  $a_c = 0.9$  with  $r_{cp} = 30dB$ , which means a larger value of  $r_{cp}$  indicates a better communication quality and a lower bit error rate. Meanwhile, when  $a_c = 0.9$  and  $\frac{P_s}{N_0} = 7dB$ , RIS-NOMA has the most considerable difference in average-BER (ABER) with NOMA-only system, indicating that RIS-NOMA localization system has better performance than NOMA-only localization system.

In Fig. 2, we compare the performance analysis of BER by RIS-NOMA system with different  $N$ . Firstly, it is observed that the ABER of the RIS-NOMA system becomes progressively decreases as  $N$  increases. Furthermore, when  $N$  is between 10 and 20, the ABER of the system falls at the fastest rate, and then the rate of decrease tends to smooth out when  $N$  is over 20.

Fig. 3 confirms that the variation of  $\overline{\sigma_{LB}}$ ,  $\overline{\sigma_t}$  with  $a_c$  for both NOMA-only and RIS-NOMA conditions, respectively. It can

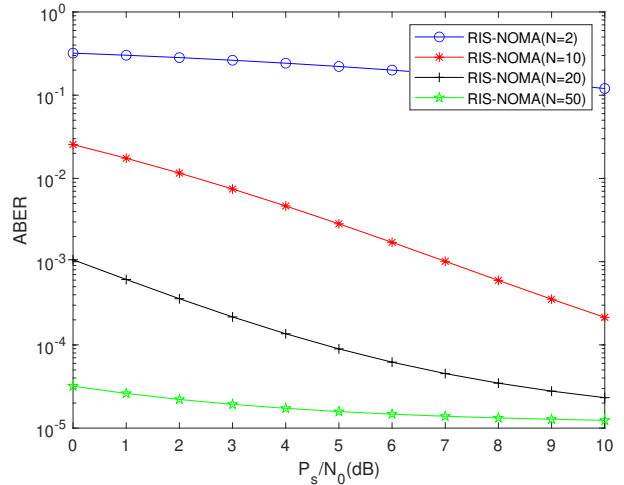


Fig. 2. Average BER vs SNR under different reflecting number  $N$ .

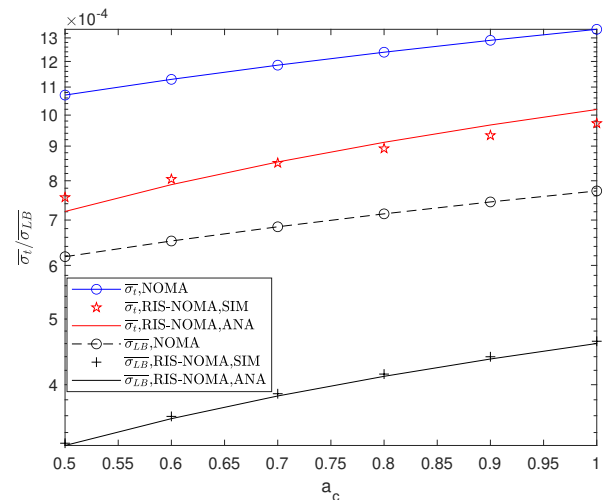


Fig. 3. CPEE/DLL Tracking error vs.  $a_c$  under different schemes.

be seen from the figure that the ranging performance of RIS-NOMA decreases with the increasing  $a_c$ . With constant  $a_c$ , the RIS-NOMA localization system outperforms the NOMA-only localization system regarding the lower bound on the estimated CPEE and the DLL tracking error.

Fig. 4 represents the estimation errors of the RIS-NOMA system with different numbers of RIS reflecting elements. From this figure, it can be seen that the system ranging performance slowly decreases with increasing  $a_c$ . As the number of RIS reflecting elements increases, the ranging performance of the system becomes better, and the lower bounds of the phase errors are all lower than the code phase measurement errors, which further indicates the stability of the model in the measurements. Finally, it can be demonstrated that our proposed RIS-NOMA localization scheme is feasible and further effectively shows that the performance of the RIS-NOMA localization system is better than that of the NOMA-

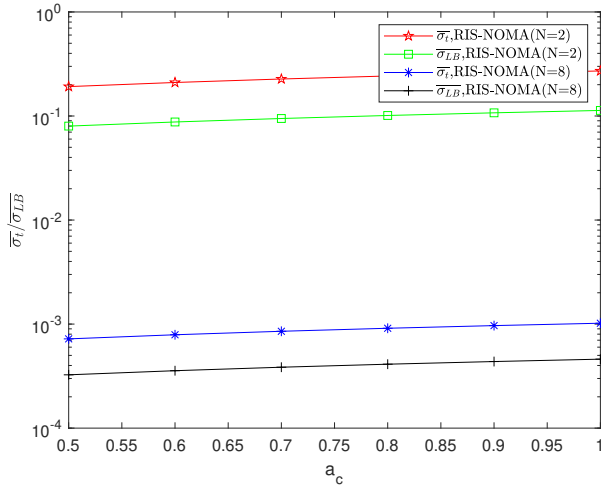


Fig. 4. CPEE/DLL Tracking error vs.  $a_c$  with different reflecting number  $N$ .

only one.

## V. CONCLUSION

In this paper, we investigate the potential of RIS to improve localization accuracy in NOMA-empowered integrated localization and communication. First, we used RIS to change the NLoS link into an LoS link; it transmitted both the localization and communication signals on this link. Then, we analysed the BER of the communication user and the CPEE of the localization user in the model. The approximate closed forms for BER, CPEE and tracking error of the DLL are derived under Rayleigh fading channels. Numerical results have been provided to validate the proposed techniques; compared with the NOMA-only localization system, the communication performance and localization performance of the RIS-NOMA localization system proposed in this paper are improved, and BER, CPEE, the tracking errors of DLL decrease with the increase of the number of RIS reflection elements.

## ACKNOWLEDGEMENT

This work is partially supported by NSFC (62001320), Central government funds for guiding local scientific and technological development of ShanXi (YDZJSX2021A037), Research Project Supported by Shanxi Scholarship Council of China (2021-133) Shanxi Province Science and Technology achievement transformation guidance special project (202204021301055).

## REFERENCES

- [1] Zhiqiang Xiao and Yong Zeng. An overview on integrated localization and communication towards 6g. *Science China Information Sciences*, 65:1–46, 2022.
- [2] Haobo Zhang, Hongliang Zhang, Boya Di, Kaigui Bian, Zhu Han, and Lingyang Song. Metalocalization: Reconfigurable intelligent surface aided multi-user wireless indoor localization. *IEEE Transactions on Wireless Communications*, 20(12):7743–7757, 2021.
- [3] Lu Yin, Jiameng Cao, Kaiqin Lin, Zhongliang Deng, and Qiang Ni. A novel positioning-communication integrated signal in wireless communication systems. *IEEE Wireless Communications Letters*, 8(5):1353–1356, 2019.

- [4] Lu Yin, Jiameng Cao, Qiang Ni, Yuzheng Ma, and Song Li. Design and performance analysis of multi-scale noma for future communication-positioning integration system. *IEEE Journal on Selected Areas in Communications*, 40(4):1333–1345, 2022.
- [5] Lincong Han, Rongke Liu, Zijie Wang, Xinwei Yue, and John S Thompson. Millimeter-wave mimo-noma-based positioning system for internet-of-things applications. *IEEE Internet of Things Journal*, 7(11):11068–11077, 2020.
- [6] Alessio Fascista, Angelo Coluccia, Henk Wymeersch, and Gonzalo Seco-Granados. Downlink single-snapshot localization and mapping with a single-antenna receiver. *IEEE Transactions on Wireless Communications*, 20(7):4672–4684, 2021.
- [7] Yiming Liu, Erwu Liu, Rui Wang, and Yuanzhe Geng. Reconfigurable intelligent surface aided wireless localization. In *ICC 2021-IEEE International Conference on Communications*, pages 1–6. IEEE, 2021.
- [8] Jiguang He, Henk Wymeersch, Long Kong, Olli Silvén, and Markku Juntti. Large intelligent surface for positioning in millimeter wave mimo systems. In *2020 IEEE 91st Vehicular Technology Conference (VTC2020-Spring)*, pages 1–5. IEEE, 2020.
- [9] Alessio Fascista, Angelo Coluccia, Henk Wymeersch, and Gonzalo Seco-Granados. Ris-aided joint localization and synchronization with a single-antenna mmwave receiver. In *ICASSP 2021-2021 IEEE International Conference on Acoustics, Speech and Signal Processing (ICASSP)*, pages 4455–4459. IEEE, 2021.
- [10] Wei Wang and Wei Zhang. Joint beam training and positioning for intelligent reflecting surfaces assisted millimeter wave communications. *IEEE Transactions on Wireless Communications*, 20(10):6282–6297, 2021.
- [11] Sha Hu, Fredrik Rusek, and Ove Edfors. Beyond massive mimo: The potential of positioning with large intelligent surfaces. *IEEE Transactions on Signal Processing*, 66(7):1761–1774, 2018.
- [12] Henk Wymeersch, Jiguang He, Benoit Denis, Antonio Clemente, and Markku Juntti. Radio localization and mapping with reconfigurable intelligent surfaces: Challenges, opportunities, and research directions. *IEEE Vehicular Technology Magazine*, 15(4):52–61, 2020.
- [13] Alexandros-Apostolos A Boulogeorgos and Angeliki Alexiou. Performance analysis of reconfigurable intelligent surface-assisted wireless systems and comparison with relaying. *IEEE Access*, 8:94463–94483, 2020.
- [14] Sarah Basharat, Syed Ali Hassan, Haris Pervaiz, Aamir Mahmood, Zhiguo Ding, and Mikael Gidlund. Reconfigurable intelligent surfaces: Potentials, applications, and challenges for 6g wireless networks. *IEEE Wireless Communications*, 28(6):184–191, 2021.
- [15] Yanyu Cheng, Kwok Hung Li, Yuanwei Liu, Kah Chan Teh, and George K Karagiannidis. Non-orthogonal multiple access (noma) with multiple intelligent reflecting surfaces. *IEEE Transactions on Wireless Communications*, 20(11):7184–7195, 2021.
- [16] Dongfang Xu, Xianghao Yu, Derrick Wing Kwan Ng, Anke Schmeink, and Robert Schober. Robust and secure resource allocation for isac systems: A novel optimization framework for variable-length snapshots. *IEEE Transactions on Communications*, 70(12):8196–8214, 2022.